RSC Advances

PAPER

View Article Online
View Journal | View Issue

Cite this: *RSC Adv.*, 2017, **7**, 851

Dual-pH-sensitivity and tumour targeting core–shell particles for intracellular drug delivery†

Weiju Hao,[a] Yinxing Shen,[a] Danyang Liu,[a] Yazhuo Shang,[a] Junqi Zhang,*[b] Shouhong Xu*[a] and Honglai Liu[a]

Received 14th October 2016
Accepted 14th November 2016

DOI: 10.1039/c6ra25224a

www.rsc.org/advances

The principal problem in the area of drug delivery is achieving better selectivity and controllability. A new core–shell nanoparticle composite (denoted MSN@Tf@Polymer) with dual-pH-sensitivity has been prepared as a drug carrier for intracellular drug delivery and release. MSN@Tf@Polymer consists of mesoporous silica nanoparticles (MSN), green-transferrin (Tf) and diblock copolymer (poly-2-diisopropylamino ethylmethacrylate-*b*-methoxy-poly ethyleneglycol: $mPEG_{45}$-$PDPA_n$). The core–shell structure is self-assembled layer by layer. Results show that nearly 80% doxorubicin hydrochloride (DOX) loaded in MSN@Tf@Polymer could be released in 5 h at pH 5.0, which is an improvement from the results obtained at pH 6.5 and pH 7.4. MTT assay and fluorescence inversion microscope experiments indicate that MSN@Tf is successfully taken up by liver cancer cells (Huh7) without apparent cytotoxicity, and Tf has strong intensity of fluorescence for subcellular localization. Confocal laser scanning microscopy (CLSM) experiments indicate that MSN@Tf@Polymer is able to enter the lysosome of the tumor cells. Furthermore, cell apoptosis experiments prove that DOX loaded in MSN@Tf@Polymer has the best anti-tumor effect compared with free DOX and DOX in bare MSN. MSN@Tf@Polymer has high biocompatibility, enhanced drug loading, site-specific delivery and *in situ* stimulus release and will also hopefully be applied as an intracellular drug delivery system.

1 Introduction

Cell apoptosis is known to be based on the drug delivery into the cell matrix, or more precisely, into the nuclei. Several carriers release their cargoes near the morbid site and then the cargoes have to undergo membrane penetration, be encapsulated in the lysosome and be released again into the matrix before reaching the nuclei.[1] On the other hand, carriers that are easily taken up by cells could deliver drugs directly inside cells.[2] Intracellular delivery and release could not only transport drugs more quickly, but also avoid lowering the activity of the effective constituents. Particularly, bare DNA, RNA or oligonucleotides that could not resist the reaction with enzymes settle in the biomembrane.[3]

In addition to their stable chemical properties, mesoporous silica nanoparticles, MSN, are often selected as drug carriers because of their tunable pore size, high surface area, and pore volume, which give them high drug loading capacity and a sustained release effect.[4] Bare MSN certainly have some shortcomings as they aggregate easily and leak drugs significantly. Therefore, modification of MSN to obtain combined structures is always considered to be a good strategy. Cui[5] *et al.* prepared a pH and thermo dual-stimuli-responsive drug carrier based on MSN@Lipid. Su[6] and co-workers reported the fabrication of Fe_3O_4@PAA/SiO_2 core–shell nanoclusters for pH-responsive drug delivery with improved blood circulation time and sustained release effect. In recent decades, the accurate delivery and regular release of anti-tumor drugs are increasingly required in order to avoid side-effects. Installing a targeting warhead on carriers/or drugs for specific cell adsorption could solve this problem. For example, the transferrin receptor[7,8] (Tf-R) is overexpressed on glioblastoma compared with normal cells. Zhang *et al.* reported[9] that nanoparticles modified by Tf could strongly interact with MCF-7 breast tumor cells through Tf-R. Chen and his group[10] also utilized Tf as the targeting ligand to vector the glioma. In addition, various functional components have been designed into nanostructures for regular releases,[11,12] which are often controlled by pH, temperature or photo irradiation. Block copolymers with various smart groups have been a developed type of strategy for drug delivery systems.[13,14] There are numerous reports about stimuli-responsive polymers[15,16] that could help achieve controllable drug release. The polymers as carriers to control the drugs loaded and released due to environmental changes[17,18] or external stimuli.[19,20] Liu designed and prepared[21]

[a]*Key Laboratory for Advanced Materials, College of Chemistry and Molecular Engineering, East China University of Science and Technology, Shanghai, 200237, China. E-mail: xushouhong@ecust.edu.cn*

[b]*Key Laboratory of Medical Molecular Virology, Ministry of Health and Ministry of Education, School of Basic Medical Sciences, Fudan University, 138 Yixueyuan Rd, Shanghai 200032, PR China. E-mail: junqizhang@fudan.edu.cn*

† Electronic supplementary information (ESI) available. See DOI: 10.1039/c6ra25224a

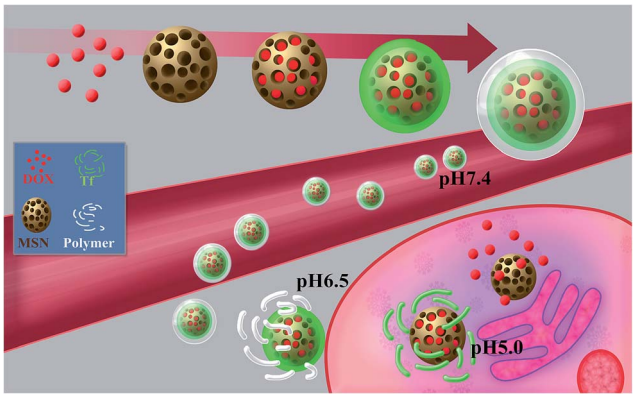

Scheme 1 Schematic of the intracellular drug delivery and release of the pH-sensitive MSN@Tf@Polymer.

poly(methacrylic acid)-grafted nanoparticles for pH-sensitive drug release. Du *et al.*[22] prepared vesicles composed of a pH-sensitive triblock polymer (PMPC–PMDA–PDPA) with variable trigger points for multi-controlled drug release. Zhou[23] reported thermo-responsive drug release from Hela cell targeted micelles formed by pluronic-poly(D,L-lactic acid). Lin[24] reported that the grafted thermo-sensitive polymer brushes, outside the HAuNs, play the role of "gate molecules" for controlled drug release. However, the problem in controllable drug delivery systems still is principally how to further achieve better selectivity and controllability.

Herein, a nanoparticle composite with a complex structure, MSN@Tf@Polymer, has been designed based on the *in situ* extra and intracellular pH. The composite structures have a smart double-shell, which is composed of green fluorescent marked transferrin (Tf) and diblock copolymer $mPEG_{45}$-$PDPA_n$ layers. The MSN acts as a core, which provides a high drug loading capacity. Tf is selected for tumour cell targeting and subcellular localization, as well as the function of sealing up the pores of MSN, whereas the self-assembled copolymer acts as a pH-controlled protective cover for Tf. The copolymer layers can rapidly collapse when the pH of the microenvironment changes to weak acidity[25,26] at the tumor site. The Tf is then exposed and the nanoparticles easily combine with the Tf receptor on cancer cells to perform a targeting action and promote endocytosis.[27] Doxorubicin hydrochloride (DOX) is used, herein, as an anticancer drug to evaluate the loading and controlled releasing behaviors[28,29] of the composite. As a result, DOX-loaded MSN@Tf enters endosomes/lysosomes[30] (pH 4.5–6.0), the Tf (isoelectric point IP = 5.9) layer is destroyed and DOX is released inside the cell (Scheme 1). The unique nanostructures prepared, herein, are expected to have fine dual-pH-sensitivity and achieve site specific delivery/release with no need for external stimuli.

2 Experimental

2.1 Materials

2-(Diisopropylamino) ethyl methacrylate (DPA, 99.5%), *N*″-pentamethyl-diethylenetriamine (PMDETA, 98%) and copper(I) bromide (CuBr, 98%) were purchased from J&K. Cetyltrimethylammonium bromide (CTAB), tetraethylorthosilicate (TEOS), 3-triethoxysilylpropylamine (KH550), polyethylene glycol ($mPEG_{45}$, M_n = 2000 g mol^{-1}, 98%) and doxorubicin hydrochloride (DOX·HCl, 98%) were purchased from Aldrich. Transferrin marked with green fluorescein (Tf) was purchased from Life Technologies Company. Tetrahydrofuran (THF, AR), methanol (AR) and methylene chloride (CH_2Cl_2, AR) were purchased from the Shanghai Taitan Company. Huh7 cells were purchased from American Type Culture Collection (ATCC). The colouration box of Cell Counting Kit-8 (CCK-8), 10% fetal bovine serum (FBS) medium and Dulbecco's modified eagle medium (DMEM, pH 7.31) were purchased from the Biotech Company of Shanghai. Green fluorescent calcein and red fluorescent propidium iodide (PI) were purchased from Beyotime Biotechnology Co. Ltd. LysoTracker Red (1 mmol L^{-1}, DMSO) and CytoTracker Red (Dil, DMSO) were purchased from Thermo Fisher Scientific.

2.2 Synthesis of $mPEG_{45}$-$PDPA_n$

$mPEG_{45}$-$PDPA_n$ (n = 100, 150 and 200, denoted as P100, P150 and P200, respectively) block copolymers were synthesized following a previously reported procedure.[31] In brief, the hydroxyl end group of $mPEG_{45}$ was first coupled to a chain transfer agent to form a macroinitiator, $mPEG_{45}$-Br. $mPEG_{45}$-Br was subsequently used to grow DPA blocks *via* atom transfer radical polymerization (ATRP). Dry CH_2Cl_2 was used as the solvent and PMDETA was used as the ligand. The mixture was degassed under liquid nitrogen, and CuBr was added as a catalyst under the protection of argon (Ar). The molar ratio of [DPA] : [PEG-Br] : [CuBr] : [PMDETA] was n:1 : 1 : 1.1. The reaction was carried out at room temperature for 12 h. The reaction solution was diluted by adding THF (about 200 mL) and passed through an alumina column (200–300 mu) to remove the catalyst. The product was obtained after precipitation by methanol. The products were verified by gel permeation chromatography (GPC, PL-GPC50) and nuclear magnetic resonance (^{1}H NMR, Bruker 400 MHz spectrometers).

2.3 Synthesis of MSN

Briefly, CTAB (0.5 g, 1.37 mmol) was dissolved in 480 mL of NaOH aqueous solution (4.2 mmol L^{-1}) and the solution was stirred at 50 °C for 30 min. Subsequently, TEOS (2.5 mL, 11.2 mmol) and KH550 (0.5 mL, 2.14 mmol) were added. To collect the formed silicon dioxide after 2 h, the solution was centrifuged at 12 000 rpm for 10 min, then washed with deionized (DI) water three times and ethanol three times, followed by vacuum drying. Extraction of residual CTAB was performed by suspending MSN in a mixture of ethanol and 37.6% HCl (160 : 1 = v/v). After stirring at 80 °C for 12 h, the purified MSN were collected by centrifugation and washed with DI water and ethanol three times. Nitrogen (N_2) adsorption and desorption analysis of MSN was conducted on a BET (Micromeritics TriStar 3000). The size and zeta potential of the nanoparticles were measured by dynamic light scattering (DLS) (Malvern, UK).

Their morphologies were observed by transmission electron microscopy (TEM, JEM-1400).

2.4 Preparation of MSN@Tf and MSN@Tf@Polymer

The formation of the layer-by-layer structure was monitored by infrared spectroscopy (FT-IR, Nicolet 380). 9 mg of MSN was added to 3 mL of PBS (pH 7.4, 1 mmol L^{-1}), followed by ultrasonic dispersion for about 30 min at room temperature. Then, various concentrations of Tf were added and the mixture was stirred overnight. The Tf adsorption ratio (AR, %) and adsorption amount (AA, mg g^{-1}) could be expressed as eqn (1) and (2):

$$\text{AR } (\%) = \frac{W_{\text{Tf}} - W_{\text{free}}}{W_{\text{Tf}}} \times 100\% \quad (1)$$

$$\text{AA } (\%) = \frac{W_{\text{Tf}} - W_{\text{free}}}{W_{\text{MSN}}} \times 100\% \quad (2)$$

where W_{Tf} and W_{free} are the weights of the original and free Tf, respectively, and W_{MSN} is the weight of the dried MSN. Furthermore, $mPEG_{45}$-$PDPA_n$ (30 mg) copolymers were dissolved in 5 mL of THF. 0.05 mL of copolymer solution was added dropwise to the MSN@Tf solution. Finally, the MSN@Tf@Polymer suspension was obtained after the THF was evaporated.

For DOX-loaded MSN@Tf@Polymer, prior to adding Tf, DOX was dissolved in PBS (pH 7.4, 1 mmol L^{-1}) with MSN and stirred for 12 h. Then, the DOX-loaded MSN@Tf@Polymer was centrifuged (12 000 rpm, 10 min) to remove the unloaded DOX. The drug-loading content (DLC) and drug-loading efficiency (DLE) were determined using eqn (3) and (4).

$$\text{DLC } (\%) = \frac{\text{weight of the drug in MSN}}{\text{weight of MSN}} \times 100 \quad (3)$$

$$\text{DLE } (\%) = \frac{\text{weight of the drug in MSN}}{\text{weight of the drug in feed}} \times 100 \quad (4)$$

The weight of the drug in MSN was determined by the difference between the weights of the drug in the feed and drug not adsorbed.

2.5 *In vitro* release of DOX

pH-controlled drug release experiments were performed in PBS in triplicate for each sample. 1 mL MSN@Tf@Polymer solution (3 mg mL^{-1}) was transferred to a dialysis bag (M_n = 14 000 Da) and immersed in 25 mL of PBS (10 mmol L^{-1}, pH 7.4, pH 6.5 and pH 5.0) at 37 °C. At predetermined time intervals (1, 2, 3, 4, 5, 7, 9, 11, 15, 20 and 24 h), the release amounts of DOX were monitored using a UV-Vis spectrophotometer (UV-vis, Shimadzu) at a wavelength of 485 nm (DOX). The cumulative release was calculated using eqn (5):

$$\text{Cumulative drug release } (\%) = \frac{M_t}{M_z} \times 100 \quad (5)$$

where M_t is the amount of DOX released from MSN@Tf@Polymer and M_z is the amount of DOX loaded in MSN@Tf@Polymer.

2.6 Cell experiments

2.6.1 Cytocompatibility. Huh7 cells and HEK293 cells purchased from ATCC were seeded in a 96-well plate at a density of 2000 cells per well. MSN@Tf@P100, MSN@Tf@P150 and MSN@Tf@P200 with different concentrations (0, 25, 50, 100, 200 and 250 μg mL^{-1}) were added to the plate. After incubation for 24 h, 10 μL of Cell Counting Kit-8 (CCK-8: 10%, no serum) was added for a further 1 h of incubation. Cell viability was determined by a microplate spectrophotometer (ELX800 Biotek, U.S.A.) at 450 nm.

2.6.2 Endocytosis. Huh7 cells were separately seeded in a 24-well plate (1×10^4 per well) and cultured in 0.5 mL of DMEM containing 10% FBS for 24 h under a humidified 5% CO_2 atmosphere. MSN@Tf@Polymer was dispersed in DMEM (100, 200 and 250 μg mL^{-1}) and cultured with cells for different times (1, 3 and 5 h) at 37 °C. The DMEM was replaced by PBS. Subsequently, endocytosis was detected by fluorescence microscopy (EVOS. AMG). The Huh7 cells were fixed by methanol (4%, mL mL^{-1}) and nuclei were stained by Dapi (blue) for 15 min. (a) The quantitative transfection efficiency of Huh7 cells and HEK293 cells was detected by flow cytometry (BD Biosciences, U.S.A.). Huh7 cells and HEK293 cells were treated with MSN@Tf and MSN@Tf@Polymer (concentration of nanoparticles: 100 μg mL^{-1}) for 3 h. The green fluorescence of Tf in the cells was detected by flow cytometry. (b) The effect of pH value on Huh7 cells was also considered. In brief, Huh7 cells were treated with MSN@Tf@P100 (concentration of nanoparticles: 100 μg mL^{-1}) for 3 h at pH 6.5, pH 7.4 and pH 8.0. Endocytosis was detected by flow cytometry. (c) Huh7 cell uptake was evaluated after the Tf receptors were blocked with different concentrations (5 μg mL^{-1}, 10 μg mL^{-1} and 20 μg mL^{-1}) of Tf. After the Huh7 cells were cultured with various concentrations of Tf for 1 h, the extra Tf was removed. Then, the Huh7 cells were cultured with MSN@Tf (100 μg mL^{-1}) for 3 h. The results were characterized by flow cytometry. These experiments were repeated at least three times.

2.6.3 Subcellular localization. Subcellular localization was detected by confocal laser scanning microscopy (CLSM). Huh7 cells were separately seeded in a 24-well plate (1×10^4 per well) and cultured in 0.5 mL of DMEM containing 10% FBS for 24 h under a humidified 5% CO_2 atmosphere. MSN@Tf@Polymer (100 μg mL^{-1}) was incubated with Huh7 cells for 3 h, and then the medium was replaced by PBS. The cytomembrane and lysosome were dyed by Dil and LysoTracker (both in red) for 30 min, respectively. After the dye was removed by PBS buffer, the nuclei were stained by Dapi (blue) for 15 min. The excitation wavelength was 358 nm for blue, 543 nm for red and 488 nm for green channels.

2.6.4 Anti-cancer effect. The morphology of Huh7 cells was investigated under different formulations of DOX (free DOX, DOX in bare MSN or MSN@Tf). Huh7 cells were incubated in a 24-well plate with DMEM for 3 h using the different doses of DOX (the relative concentrations of DOX were fixed to be 0, 5, 10 and 25 μg mL^{-1}). Then, DMEM was replaced by fresh PBS and the cells were cultured for another 21 h. The cells were treated with 2 μM calcein-AM and 4.5 μM PI for 30 min. Living cells

were stained green and dead cells were stained red. The images were observed by fluorescence microscopy at 450 nm. The quantitative viability of Huh7 cells was detected by CCK-8 (MTT).

2.6.5 Cell apoptosis. Quantitative measurements of cell apoptosis were made using flow cytometry. Huh7 cells cultured in a 24-well plate were treated with different formulations of DOX (free DOX, DOX in MSN or MSN@Tf, relative concentration of DOX: 10 μg mL^{-1}) at 37 °C for 3 h. Then, fresh DMEM was added and the cells were cultured. After further culture for 21 h, the cells were rinsed with PBS 2 times and detached using a trypsin–EDTA solution. Cell apoptosis was then analyzed on a flow cytometer.

3 Results and discussion

3.1 Synthesis of the pH-sensitive $mPEG_{45}$-$PDPA_n$

pH-sensitive diblock copolymers, $mPEG_{45}$-$PDPA_n$ (n = 100, 150 and 200), were synthesized. The chemical structures of $mPEG_{45}$, $mPEG_{45}$-Br and P100 ($mPEG_{45}$-$PDPA_{100}$) were confirmed by ^1H NMR (S1†). Their molar weights obtained by ^1H NMR ($M_{n,NMR}$) and GPC $M_{n,GPC}$ are listed in Table 1. These results indicate that the target copolymers we successfully obtained.

The pH-sensitivities of the copolymers were investigated by measuring their transmittance and zeta-potentials. As shown in Fig. 1, below pH 5.0, the transmittance of the copolymer solutions was about 100% and their zeta potentials were all more than +25 mV, which reveal that the copolymers could dissolve completely under these conditions. The copolymers were found to be sensitive to the shocks of NaOH addition due to the deprotonation of the PDPA block. The triggering pH values were decided by the pH at which the solutions showed a sudden change in transmittance in the pH range of 6.4–7.0 (Table 1). With an increase in pH, the zeta potentials became lower and the isoelectric points (IP) were in the pH range of 6.9–7.5 (Fig. 1b), which are almost consistent with the pH values at which aggregation of the copolymer occurs (Fig. 1a).

3.2 Characterization of MSN, MSN@Tf and MSN@Tf@Polymer

The nitrogen (N_2) adsorption and desorption isotherms of MSN were measured by BET. The surface area and pore size of MSN were 657.3 m^2 g^{-1} and 2.3 nm, respectively (Fig. S2†). The IP value of Tf was found to be pH 5.9, as shown in Fig. S3.† The intensities of the UV-Vis absorption peak at 280 nm of Tf were used to estimate the amount of Tf adsorbed according to a standard calibration curve (Fig. S4†). Table S1† shows the values of AR and AA with Tf concentration. With an increase in Tf concentration, the AA value of Tf increased from 2.5 to 175 mg g^{-1}. The adsorption of Tf reached a saturated state when the concentration of Tf was 2.0 mg mL^{-1}.

The properties and parameters of Tf, copolymer and MSN@Tf@Polymer are shown in Table 2. MSN modified with $-NH_2$ groups showed a strong positive potential, whereas the free Tf was negatively charged. The multi-layer shell on the MSN surface was structured layer by layer *via* mixing MSN with Tf and polymer successively. MSN and Tf were mixed in different ratios and MSN@Tf was formed through electrostatic forces. Then, the amphiphilic copolymers were added and self-assembled around MSN@Tf to form a second layer.

Fig. 2a shows the zeta-potentials of bare MSN, Tf, MSN@Tf, copolymer and MSN@Tf@Polymer. After being assembled layer by layer, the surface charge of MSN changed from +37.1 mV (bare MSN) to about +24.4 mV (3@1.0) and +7.4 mV (3@1.0@0.1) at pH 7.4. The TEM images shown in Fig. 2b display spherical MSN with well-ordered channels (Fig. 2b, Left). After mixing with Tf and copolymer, the pore structure

Table 1 Properties of the synthesized di-block copolymers. $M_{n,T}$ is the calculated molar weight and X_c is the percentage of conversion

Polymer	Composition	$M_{n,T}$ (g mol^{-1})	X_c	$M_{n,NMR}$ (g mol^{-1})	$M_{n,GPC}$ (g mol^{-1})	PDI	Triggering pH
P100	$mPEG_{45}$-$PDPA_{100}$	23 332	95%	22 165	21 567	1.19	6.4
P150	$mPEG_{45}$-$PDPA_{150}$	33 998	88%	29 918	27 742	1.22	6.7
P200	$mPEG_{45}$-$PDPA_{200}$	44 664	86%	38 411	37 236	1.22	7.0

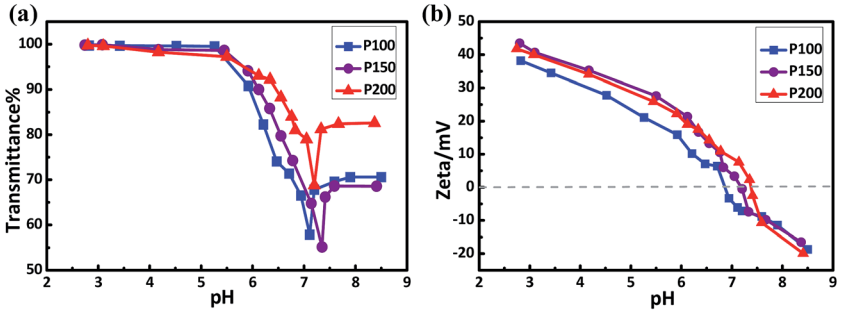

Fig. 1 pH-sensitivities of the copolymers as detected by UV-vis spectroscopy (a) and DLS (b). The concentration of the copolymer was 0.1 mg mL^{-1}.

Table 2 Properties and parameters of MSN, copolymer, MSN@Tf and MSN@Tf@P100 under PBS (pH 7.4)

Component	Concentration (mg mL^{-1})	Diameter (nm)	PDI	Zeta (mV)
MSN	3.0	110 ± 4	0.022	+37.1
Tf	0.1	11 ± 1	0.500	−26.1
	0.5			
	1.0			
P100	0.1	7.0 ± 2	0.350	−7.7
MSN@Tf	3@0.01	135 ± 5	0.200	+36.8
	3@0.05			+36.2
	3@0.1			+32.5
	3@0.5			+30.5
	3@1.0			+24.4
	3@2.0			+16.6
	3@3.0			+14.5
MSN@Tf@P100	3@1.0@0.1	170 ± 5	0.224	+7.4

became blurry and a gradually thickened shell appeared outside MSN, which suggests the formation of a multi-layer structure. Furthermore, infrared spectra were obtained to confirm the composition of the constructed MSN@Tf@Polymer. Fig. 2c shows the characteristic peaks of –NH_2 at 3436 cm^{-1} and 3465 cm^{-1} for MSN and MSN@Tf, respectively. The peaks at 2931 cm^{-1} and 1126 cm^{-1} are attributed to –CH_3 and–CH–$(CH_3)_2$ on the copolymer, respectively. Fig. 2d shows the sizes of the samples obtained by DLS, which are consistent with those estimated from the TEM images. These results indicate that Tf and the copolymer successfully covered the surface of MSN.

3.3 DOX release of MSN and MSN@Tf@Polymer

The pH-controlled drug release of the core–shell MSN@Tf@Polymer was investigated for various pH values using DOX as the model drug. The DLC value of MSN was about 80% and the DLE was about 66 μg mg^{-1}. Three pH values (pH 7.4, 6.5 and 5.0) were selected, which simulated the pH value of normal body blood, tumor extracellular and endosome matrix.[32] Then, the DOX release processes of MSN and MSN@Tf@Polymer were monitored within 24 h at 37 °C. As shown in Fig. 3a, the DOX released amounts of MSN increased a little with a decrease in pH value during the first 5 h and stopped when the release amount reached 80%. Particularly in the first hour,

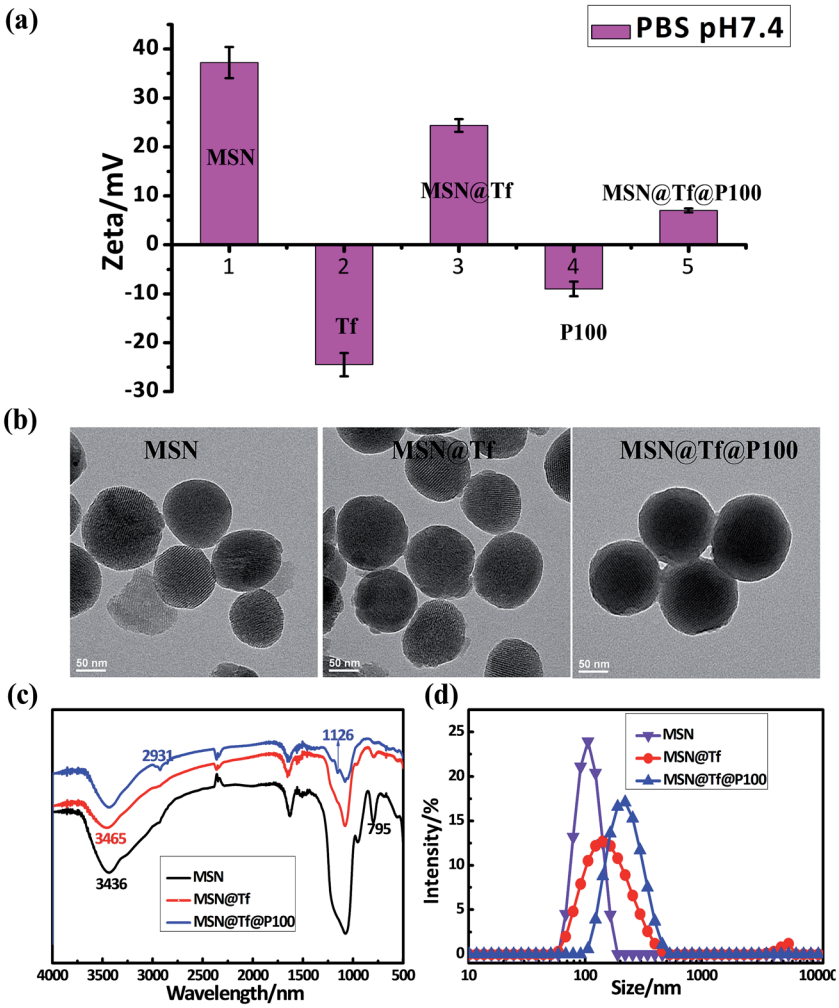

Fig. 2 Zeta potentials of (a) MSN, Tf, MSN@Tf (3@1.0), P100 and MSN@Tf@P100 (3@1.0@0.1) and their TEM images (b), FT-IR spectra (c) and sizes (d) in PBS (pH 7.4).

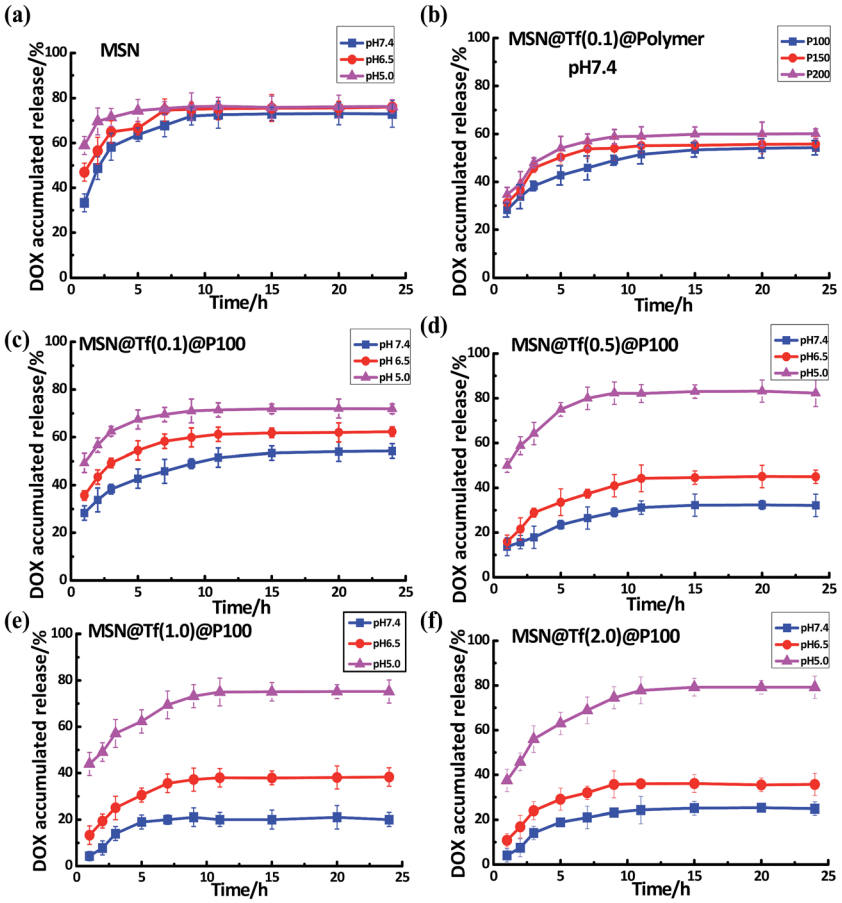

Fig. 3 DOX release of the various MSN@Tf@Polymers at pH 7.4, pH 6.5 and pH 5.0 (37 °C). (a) Drug release of bare MSN (3 mg mL^{-1}) at various pH values; (b) drug release of MSN@Tf@Polymer covered by different types of copolymers at pH 7.4; and (c), (d), (e) and (f) drug release of MSN@Tf@Polymer prepared using Tf concentrations of 0.1, 0.5, 1.0 and 2.0 mg mL^{-1}, respectively.

more than 30% of DOX was released at pH 7.4, which suggests that the leakage of DOX from the bare MSN was significant. The increase in DOX leakage with a decrease in pH is thought to be related to the better dissolving capacity of DOX in acidic condition. Fig. 3b shows that MSN@Tf@P100 had the lowest DOX leakage at pH 7.4 among the three copolymers, which is considered to be relative to the triggering pH point of the copolymers. As shown in Table 1, the triggering pH increased from 6.4 to 7.0 when PDPA was lengthened. Then, copolymers P200 and P150 were somewhat protonated at pH 7.4, which resulted in an unstable copolymer layer.

Fig. 3c–f show the DOX release under various pH values from MSN@Tf@P100 covered by different concentrations of Tf. Tf was used to block the pores of MSN and decrease drug leakage before delivery to the destination. As shown in Fig. 3c–f, with an increase in the Tf adsorption amount, the leakage of DOX at pH 7.4 decreased until the Tf concentration became 1.0 mg mL^{-1}. At this concentration, MSN appeared to be covered by enough Tf and achieve a good sealing effect. As shown in Fig. 3e, at pH 7.4, less than 15% of DOX was released from MSN@Tf@P100 during the first 3 h. It was reported that 2–3 h was a sufficient time period for cell transfection,[33] and therefore the MSN@Tf@Polymer

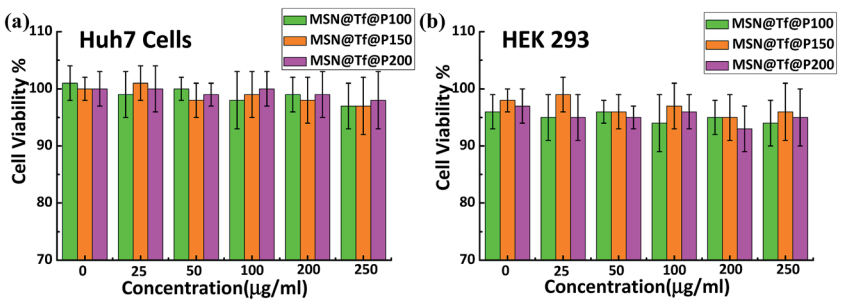

Fig. 4 Huh7 cells (a) and HEK293 cells (b) cultured with different concentrations of MSN@Tf@Polymer for 24 h (pH 7.4).

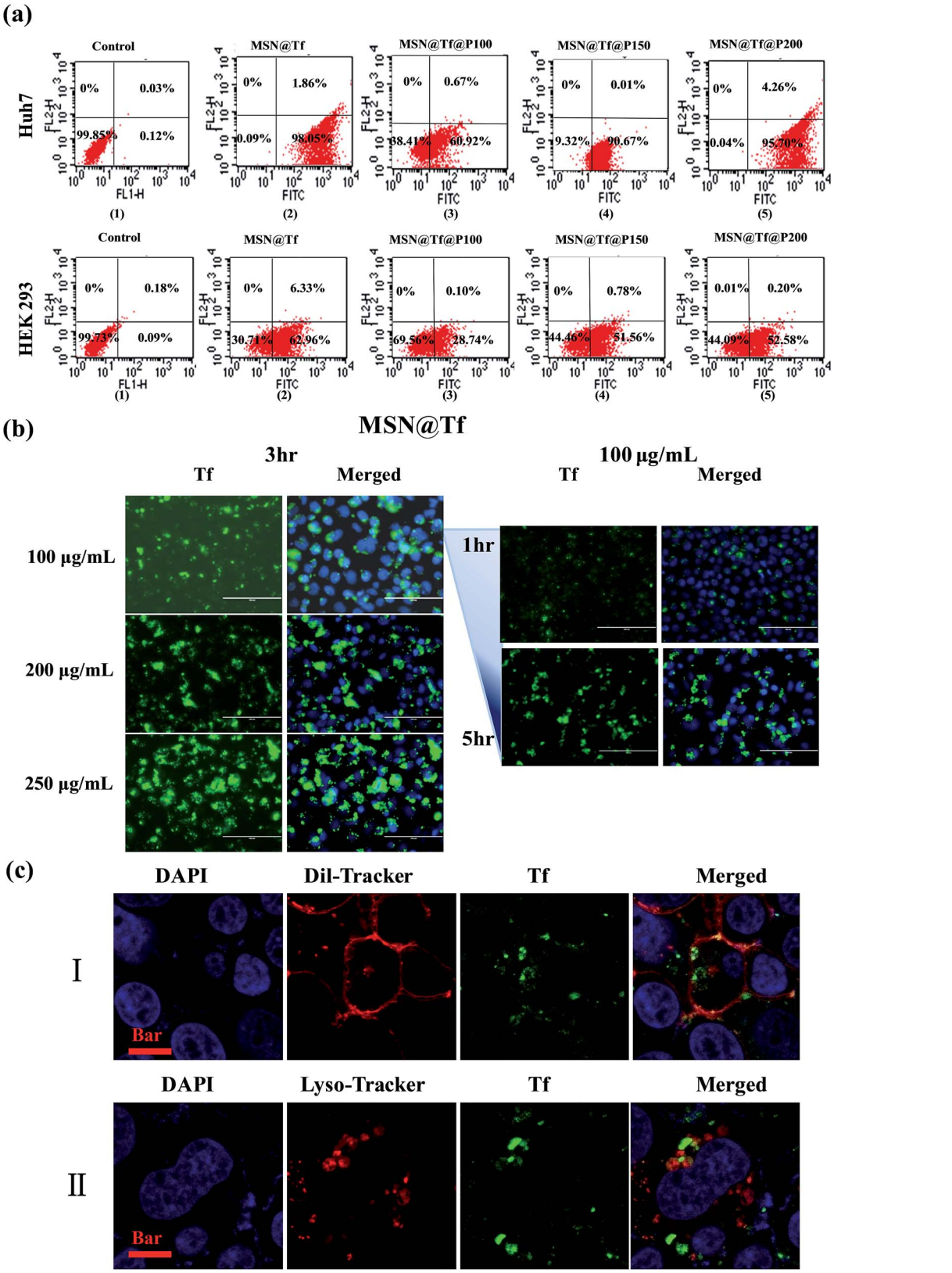

Fig. 5 Cell uptake and distribution of MSN(3.0)@Tf(1.0)@Polymer(0.1) in Huh7 cells or HEK 293 cells. (a) Flow cytometry quantitative analysis of Huh7 cells or HEK 293 cells uptake of various samples after culture for 3 h. The *Control* was the cells cultured with DMEM only. (b) Fluorescence images of green and merged fluorescence of green and blue. Left: cells were incubated with MSN@Tf (100, 200 and 250 μg mL^{-1}) for 3 h. Right: cells were incubated with MSN@Tf (100 μg mL^{-1}) for different times (1 and 5 h). The bar is 200 μm. (c) CLSM images of Huh7 cells cultured with MSN@Tf@P100 for 3 h. Red fluorescence in (I) cytomembrane; red fluorescence in (II) lysosome. For all images: Blue: nuclei and green: Tf. The bars are 10 μm.

prepared, herein, could be expected to achieve intracellular drug delivery[34] and release. With a decrease in pH, the DOX release amounts were found to increase by various degrees. When pH decreased to 6.5, the PDPA blocks were protonated and the copolymer layer collapsed. Moreover, the Tf layer became somewhat flexible under the weak acidic condition due to mild protonation. The DOX release amount at this pH increased a little more than that at pH 7.4. As expected, the DOX release became very quick when the pH decreased to 5.0, since at this pH the Tf layer fell off from MSN due to the disappearance of the electrostatic interaction between MSN and Tf. Then, the maximum release amount reached close to 80%, similar to bare MSN. In the following cell experiments, the MSN@Tf@Polymer prepared with MSN (3 mg mL^{-1}), Tf (1.0 mg mL^{-1}) and copolymer (0.1 mg mL^{-1}) was chosen.

3.4 Cytocompatibility assay

The short-term cytotoxicity of MSN(3.0)@Tf(1.0)@Polymer(0.1) was evaluated by an MTT assay firstly. As shown in Fig. 4, the MSN@Tf@Polymer had no evident cytotoxicity to Huh7 and HEK293 cells in the concentration range of 0–250 μg mL^{-1} after it was cultured with the cells for 24 h. The cytotoxicity of bare MSN and MSN@Tf was also investigated and similar results were obtained (not shown). These results indicate that MSN@Tf@Polymer has good potential for biomedical application.

3.5 Cellular uptake and intracellular localization

To investigate the functions of Tf and copolymer in each step of the cell transfection process, flow cytometry quantitative analysis was conducted. Huh7 tumor cell lines were incubated with MSN@Tf, MSN@Tf@P100, MSN@Tf@P150 and MSN@Tf@P200. As shown in Fig. 5a, the strongest fluorescent intensity signal inside the cells was observed when cultured with MSN@Tf. The transfection efficiency of MSN@Tf was about 98.05%, which suggests the tumor-targeting function of the Tf adsorption layer. Unexpectedly, MSN@Tf@P150 and MSN@Tf@P200 also had high transfection efficiencies, which were about 90.67% and 95.70%, respectively. This is considered to be related to the pH of the culture medium, which was found to decrease to less than pH 7.0 due to cell metabolism. P150 and P200 are slightly protonated at pH 7.4, as mentioned above, and protonated even further with a decrease in pH. The high transfection of MSN@Tf@P150 and MSN@Tf@P200 indicates that the copolymer layer might collapse during culture with cells. P100 had a pH-trigger point of about 6.4 (Table 1), and its slower protonation allowed Tf to be shielded by the copolymer layer for a longer time, which resulted in a lower transfection efficiency of about 60.92%. For comparison with tumour liver cells, we used HEK293 cells to measure the uptake and distribution of MSN(3.0)@Tf(1.0)@Polymer(0.1). Flow cytometry quantitatively characterized the cell uptake of various samples after culture for 3 h. The cells cultured with only DMEM was the control. As shown in Fig. 5a (down), the HEK293 cells had a moderately low uptake rate because they also had Tf receptors. Moreover, the uptake rates of MSN@Tf@Polymer in HEK293 were only 28.74%, 51.56% and 52.58%, which were much lower than that of the Huh7 cells. These results indicate that the self-assembled copolymer layer has an important role in keeping the drug carrier from entering normal cells.

Since the copolymer layer was expected to collapse outside the cells, MSN@Tf was used directly in the confocal microscopy experiments to confirm cellular uptake and intracellular localization. Various concentrations of MSN@Tf were incubated with Huh7 cells for 1–5 h at 37 °C. The cell nuclei were dyed blue by DAPI. The images in Fig. 5b (Left) show an increase in green fluorescence inside the cells with an increase in the concentration of MSN@Tf after incubation for 3 h. Furthermore, 100 μg mL^{-1} of MSN@Tf was incubated with Huh7 cells for different times (1, 3 and 5 h), which are also shown in Fig. 5b (Right). It could be found that the 3 h period of time appeared to be sufficient for MSN@Tf to be transfected into cells.

To confirm the localization of MSN@Tf, Huh7 cells were incubated with MSN@Tf again for intracellular localization investigations. The cytomembrane and lysosome were both

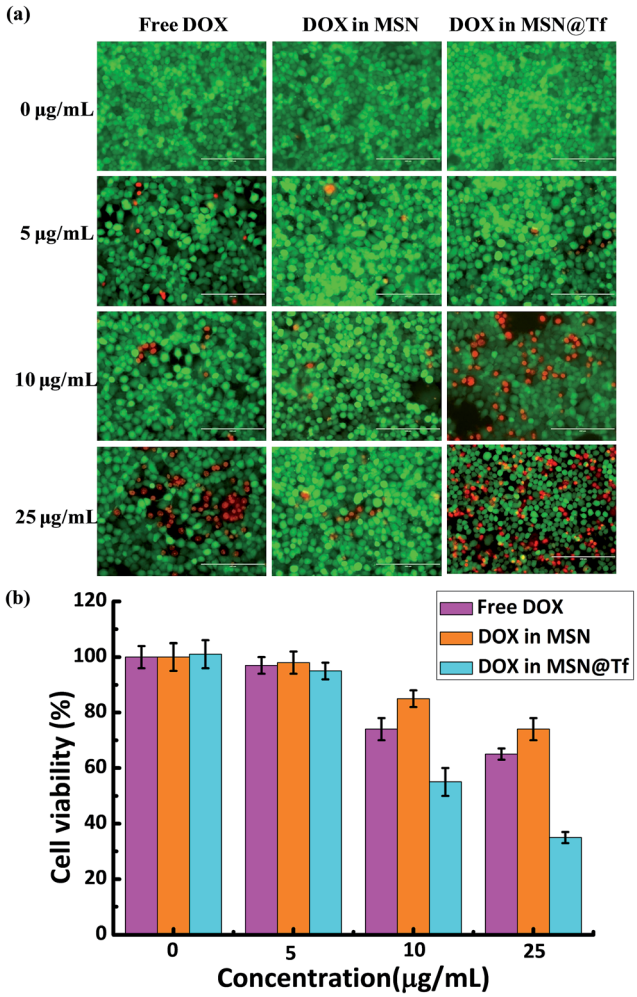

Fig. 6 (a) Visual images of Huh7 cell viability after incubation with different DOX formulations (concentration of DOX: 0–25 μg mL^{-1}) for 3 h and normal culture for a further 21 h. Green calcein-AM fluorescence and red PI fluorescence indicate live and dead cells, respectively. The bar is 200 μm. (b) Quantitative viability of Huh7 cells after incubation with different DOX formulations.

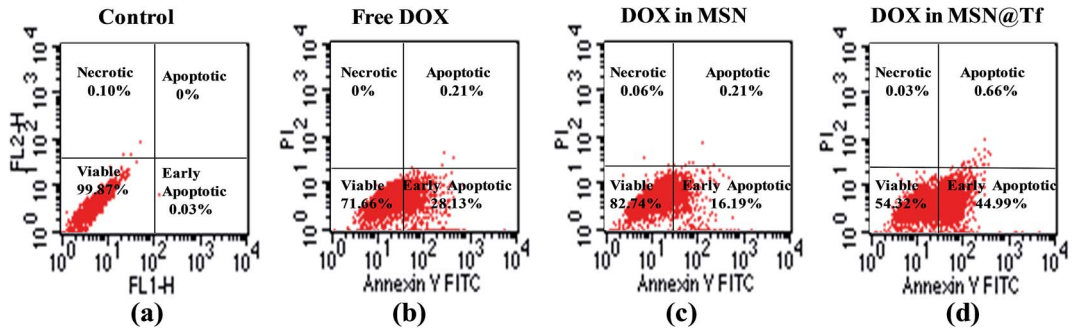

Fig. 7 Flow cytometry analysis of necrosis of Huh7 cells after treatment with PBS and DOX (10 μg mL^{-1}) in various formulations at 37 °C.

dyed red, as shown in Fig. 5c–I and II. From Fig. 5c, green fluorescence could be observed inside the cell (I) or overlapped with red fluorescence. These results suggest that MSN@Tf was taken up by the cell and entered into the lysosome. It is worth mentioning that the pH of the endosome/lysosome matrix is reported to be 4.5. Thus, MSN@Tf could release its cargo quickly at this low pH value.

3.6 Anti-cancer effect

The cytotoxicity of various DOX formulations was tested after incubating Huh7 cells with free DOX, DOX in MSN and DOX in MSN@Tf for 3 h. The green/red (live/dead) staining images are shown in Fig. 6a. DOX loaded in bare MSN had the highest cell viability, which is thought to be related to two factors: more extracellular DOX leakage and lower transfection efficiency of MSN. The DOX release amount of MSN was shown in Fig. 3a, which was found to reach up to 65% (pH 6.5) during the first 3 h. Comparing the results of free DOX, the lower cell killing capacity of DOX in MSN also illustrates that the bare MSN could hardly be internalized by cells. The Tf on MSN@Tf seemed to improve the cell transfection significantly. Then, DOX in MSN@Tf was found to be the most effective formulation for killing Huh7 cells. Fig. 6b shows the quantitative viability of Huh7 cells. These results are consistent with those in Fig. 6a and demonstrate again that free DOX and DOX in MSN are less cytotoxic. These results also confirm that Tf has the preferable ability of tumor-targeting and improves the cellular internalization of MSN@Tf.

3.7 Cell apoptosis

Flow cytometry analysis was used to investigate cell apoptosis quantitatively after treatment with PBS and DOX in various formulations. Cells incubated with PBS at 37 °C for 3 h (Control) (Fig. 7a) had a cell viability of 99.87%, which indicates that the experimental conditions used here did not cause any harm to the cells. The percentage of cell apoptosis after incubation with free DOX, DOX in MSN and DOX in MSN@Tf was 28.13% ± 1.41%, 16.19% ± 2.70% and 44.99% ± 4.23%, respectively (Fig. 7b–d). These results are well in accordance with those obtained *via* fluorescence microscopy (Fig. 6) and prove again the advantage of the MSN@Tf@Polymer prepared in this study as a tumor-targeted drug delivery system.

4 Conclusion

In summary, we have developed a tumor-targeted and pH-controllable drug delivery system, which has been constructed by the self-assembly of MSN, Tf and block copolymers ($mPEG_{45}$-$PDPA_n$). $mPEG_{45}$-$PDPA_n$ possesses high pH-sensitivity with a pH-trigger point of about 6.4–7.0 depending on the size of PDPA. The copolymers protect Tf from being degraded by bio-enzymes and improve the circulation time in the blood, whereas the Tf layer plays both sealing and targeting roles. *In vitro* DOX release experiments show that the release of DOX from MSN@Tf@Polymer decreased to a large extent due to the coverage of Tf@Polymer. MSN@Tf@Polymer possesses excellent cyto-compatibility and could be internalized into the lysosome. The acidic condition of the lysosome matrix triggers Tf to leave the MSN surface and then release DOX. Cell apoptosis experiments prove that DOX loaded in MSN@Tf@Polymer has best anti-cancer effect compared with free DOX and DOX in MSN, which suggests that the achievement of intracellular drug delivery and release has a very important significance. This dual-pH-sensitive system is expected to achieve site specific delivery/release with no need for external stimuli, which might have potential applications in the future field of gene treatment.

Author contributions

Weiju Hao and Yinxing Shen equally contributed to this work.

Conflict of interest

The authors declare no competing financial interest.

Acknowledgements

Financial support for this study is provided by the National Natural Science Foundation of China (No. 21276074), the 111 Project (No. B08021) of China and the Fundamental Research Funds for the Centre Universities of China.

References

1 M. Karimi, A. Ghasemi, P. Sahandi Zangabad, R. Rahighi, S. M. Moosavi Basri, H. Mirshekari, M. Amiri, Z. Shafaei

Pishabad, A. Aslani, M. Bozorgomid, D. Ghosh, A. Beyzavi, A. Vaseghi, A. R. Aref, L. Haghani, S. Bahrami and M. R. Hamblin, *Chem. Soc. Rev.*, 2016, **45**, 1457–1501.
2 W. J. Tipping, M. Lee, A. Serrels, V. G. Brunton and A. N. Hulme, *Chem. Soc. Rev.*, 2016, **45**, 2075–2089.
3 Q. Hu, P. S. Katti and Z. Gu, *Nanoscale*, 2014, **6**, 12273–12286.
4 L. Lu, Y. Qian, L. Wang, K. Ma and Y. Zhang, *ACS Appl. Mater. Interfaces*, 2014, **6**, 1944–1950.
5 X. Wu, Z. Wang, D. Zhu, S. Zong, L. Yang, Y. Zhong and Y. Cui, *ACS Appl. Mater. Interfaces*, 2013, **5**, 10895–10903.
6 L. Chen, L. Li, L. Zhang, S. Xing, T. Wang, Y. A. Wang, C. Wang and Z. Su, *ACS Appl. Mater. Interfaces*, 2013, **5**, 7282–7290.
7 J. Wang, S. Tian, R. A. Petros, M. E. Napier and J. M. DeSimone, *J. Am. Chem. Soc.*, 2010, **132**, 11306–11313.
8 L.-C. Wu, L.-W. Chu, L.-W. Lo, Y.-C. Liao, Y.-C. Wang and C.-S. Yang, *ACS Nano*, 2013, **7**, 365–375.
9 W. Du, Y. Fan, B. He, N. Zheng, L. Yuan, W. Dai, H. Zhang, X. Wang, J. Wang, X. Zhang and Q. Zhang, *Mol. Pharm.*, 2015, **12**, 1467–1476.
10 F. Liu, L. Wang, H. Wang, L. Yuan, J. Li, J. L. Brash and H. Chen, *ACS Appl. Mater. Interfaces*, 2015, **7**, 3717–3724.
11 M. Shao, F. Ning, J. Zhao, M. Wei, D. G. Evans and X. Duan, *J. Am. Chem. Soc.*, 2012, **134**, 1071–1077.
12 N. Lee, H. R. Cho, M. H. Oh, S. H. Lee, K. Kim, B. H. Kim, K. Shin, T. Y. Ahn, J. W. Choi, Y. W. Kim, S. H. Choi and T. Hyeon, *J. Am. Chem. Soc.*, 2012, **134**, 10309–10312.
13 O. Parlak, M. Ashaduzzaman, S. B. Kollipara, A. Tiwari and A. P. Turner, *ACS Appl. Mater. Interfaces*, 2015, **7**, 23837–23847.
14 S.-M. Lee and S. T. Nguyen, *Macromolecules*, 2013, **46**, 9169–9180.
15 A. W. Du and M. H. Stenzel, *Biomacromolecules*, 2014, **15**, 1097–1114.
16 K. Wang, Y. Liu, C. Li, S.-X. Cheng, R.-X. Zhuo and X.-Z. Zhang, *ACS Macro Lett.*, 2013, **2**, 201–205.
17 K. Knop, D. Pretzel, A. Urbanek, T. Rudolph, D. H. Scharf, A. Schallon, M. Wagner, S. Schubert, M. Kiehntopf, A. A. Brakhage, F. H. Schacher and U. S. Schubert, *Biomacromolecules*, 2013, **14**, 2536–2548.
18 L. Li and S. Thayumanavan, *Langmuir*, 2014, **30**, 12384–12390.
19 J. Song, L. Cheng, A. Liu, J. Yin, M. Kuang and H. Duan, *J. Am. Chem. Soc.*, 2011, **133**, 10760–10763.
20 D. Kurzbach, V. S. Wilms, H. Frey and D. Hinderberger, *ACS Macro Lett.*, 2013, **2**, 128–131.
21 C. L. Lay, H. R. Tan, X. Lu and Y. Liu, *Chemistry*, 2011, **17**, 2504–2509.
22 J. Du, L. Fan and Q. Liu, *Macromolecules*, 2012, **45**, 8275–8283.
23 X. Guo, D. Li, G. Yang, C. Shi, Z. Tang, J. Wang and S. Zhou, *ACS Appl. Mater. Interfaces*, 2014, **6**, 8549–8559.
24 X. Deng, Y. Chen, Z. Cheng, K. Deng, P. Ma, Z. Hou, B. Liu, S. Huang, D. Jin and J. Lin, *Nanoscale*, 2016, **8**, 6837–6850.
25 Y. Zhao, L. Cao, J. Ouyang, M. Wang, K. Wang and X. H. Xia, *Anal. Chem.*, 2013, **85**, 1053–1057.
26 N. Wang, Y. Feng, L. Zeng, Z. Zhao and T. Chen, *ACS Appl. Mater. Interfaces*, 2015, **7**, 14933–14945.
27 R. Duncan and S. C. Richardson, *Mol. Pharm.*, 2012, **9**, 2380–2402.
28 H. Li, Y. Cui, J. Sui, S. Bian, Y. Sun, J. Liang, Y. Fan and X. Zhang, *ACS Appl. Mater. Interfaces*, 2015, **7**, 15855–15865.
29 X. Jia, X. Zhao, K. Tian, T. Zhou, J. Li, R. Zhang and P. Liu, *Biomacromolecules*, 2015, **16**, 3624–3631.
30 X. Liu, B. Chen, X. Li, L. Zhang, Y. Xu, Z. Liu, Z. Cheng and X. Zhu, *Nanoscale*, 2015, **7**, 16399–16416.
31 T. Xia, W. Hao, Y. Shang, S. Xu and H. Liu, *Int. J. Polym. Sci.*, 2016, **2016**, 1–10.
32 Z. Li, J. C. Barnes, A. Bosoy, J. F. Stoddart and J. I. Zink, *Chem. Soc. Rev.*, 2012, **41**, 2590–2605.
33 J. Logie, S. C. Owen, C. K. McLaughlin and M. S. Shoichet, *Chem. Mater.*, 2014, **26**, 2847–2855.
34 L. Dai, Q. Zhang, J. Li, X. Shen, C. Mu and K. Cai, *ACS Appl. Mater. Interfaces*, 2015, **7**, 7357–7372.